Carbohydrate Polymers 92 (2013) 529–533

Contents lists available at SciVerse ScienceDirect

Carbohydrate Polymers

journal homepage: www.elsevier.com/locate/carbpol

Galectin 3–β-galactobiose interactions

A.P. Gunning, C. Pin, V.J. Morris*

Institute of Food Research, Norwich Research Park, Norwich NR4 7 UA, UK

ARTICLE INFO

Article history:
Received 11 May 2012
Received in revised form 23 August 2012
Accepted 26 August 2012
Available online 2 September 2012

Keywords:
Modified pectin
Gal3
Anti-cancer action
β-Galactobiose
Force spectroscopy
Atomic force microscopy

ABSTRACT

Force spectroscopy has been used to investigate the interaction between the disaccharide β-galactobiose and the pro-metastatic regulatory protein galectin-3 (Gal3). The studies revealed specific interactions characterised by an off-rate dissociation constant $k_{off} = 0.33\ s^{-1}$ and interaction distance $x = 0.2$ nm at zero applied force. These data suggest a lifetime for the interaction of 3.0 s. The results are consistent with the hypothesis that oral consumption of modified citrus pectin controls cancer metastasis by inhibiting the role of Gal3. The modification is considered to facilitate binding of pectin-derived galactan sidechains to Gal3 and inhibition of the roles of Gal3 as a pro-metastatic regulatory protein.

1. Introduction

Pectin is a complex polysaccharide component of the cell walls of non-graminaceous plants (Ridley, O'Neill, & Mohnen, 2001). Commercial pectins are extracted from the waste plant material remaining after the extraction of juice (apple pomace or citrus peel) or sugar (sugar beet pulp). The main industrial applications of citrus or apple pectin are as gelling or thickening agents, or for fermented milk drinks and similar products in which protein is suspended under the condition of relatively low pH. Extracts of pectin from sugar beet are poor gelling agents but show interesting potential industrial roles as emulsifiers. There is a growing interest in the role of modified forms (MCP) of citrus pectin as natural materials for controlling and treating cancer metastasis (Glinsky & Raz, 2009). It has been suggested that MCP acts by inhibiting the role of the pro-metastatic regulatory protein galectin-3 (Gal3).

Gal3 is the most versatile member of a family of evolutionary-conserved galactose-binding lectins (galectins) widely found in a range of species from lower invertebrates to mammals (Barondes, Castronovo, et al., 1994; Barondes, Cooper, Gitt, & Leffler, 1994). At present 15 members of this family have been identified (Gal1–15) and 10 of the proteins are human galectins (Gal1–4, 7–10, 12 and 13). Gal3 (also known as CBP35, MAC2 and IgE BP) is a 30 kDa chimeric 'tadpole-like' protein (Birdsall et al., 2001) consisting of a long thin 'collagen-like' tail at the N-terminus, and a globular structure at the C-terminus, containing a ~14 kDa carbohydrate recognition domain (Barondes, Castronovo, et al., 1994; Barondes, Cooper, et al., 1994). Through the use of solid-phase binding assays and inhibition assays several natural ligands have been identified that bind to galectins (Sörme et al., 2005). Examples include galactose, lactose, polylactosamine, and N-acetyllactosamine (LacNAc). X-ray data (Collins, Hidari, & Blanchard, 2007; Nesmelova, Dings, & Mayo, 2008, chap. 3; Seetharaman et al., 1998; Sörme et al., 2005) obtained on complexes of Gal3–lactose, Gal3–LacNAc, and Gal3–LacNAc derivatives have revealed the nature of binding of the terminal galactose residue within the primary binding site. Hydrogen bonding to O4 and O6 of the galactose and to O3 of the glucose has been found to be important for stabilising lactose-based structures within the carbohydrate recognition domain.

Citrus pectin extracts are composed of two main types of structural elements: homogalacturonans (HG-smooth regions) and rhamnogalacturonan I (RGI-hairy regions). Homogalacturonans are essentially linear homopolymers composed of partially methyl-esterified (1 → 4) linked α-D-galacturonic acid residues (Gal*p*A). The RG1 units consist of a backbone based on a repeating disaccharide [→4)-α-D-Gal*p*A-(1 → 2)-α-L-Rha*p*-(1-)] of galacturonic acid and rhamnose (Rha*p*) residues. Attached to some of the Rha*p* residues are neutral sugar sidechains consisting mainly of α-L-arabinose (Ara*f*) and/or β-D-galactose (Gal*p*) residues. Structural studies (Yapo, Lerouge, Thibault, & Ralet, 2007) on neutral sugar side chains, enzymatically released from extracts of citrus pectin RGI, have shown that combined use of endo-1,5-α-L-arabinanase, endo-1,4-β-D-galactanase, α-L-arabinofuranosidase, and β-D-galactosidase can be used to debranch the RGI sample. This

* Corresponding author. Tel.: +44 1603 255271; fax: +44 1603 507723.
E-mail address: vic.morris@ifr.ac.uk (V.J. Morris).

0144-8617/$ – see front matter © 2012 Elsevier Ltd. All rights reserved.
http://dx.doi.org/10.1016/j.carbpol.2012.08.104

suggests that citrus pectin contains β(1 → 4)-D-arabinogalactan and/or galactan side chains.

The two main types of modified pectin that have been investigated in detail are GCS-100 and Pectasol-C. GCS-100 is modified by chemical treatment: originally the pectin was first alkali-treated and then acid-treated to lower the molecular weight to ∼10 kDa (Raz & Pienta, 1998). Some publications refer to an additional heat treatment, although the details and structural implications are unclear. In at least one study (Wang, Nangia-Makker, Balan, & Raz, 2010) the term GCS-100/MCP is used to describe a product produced from citrus pectin apparently just involving a heat (autoclaving) treatment. Pectasol-C is prepared by enzymatic treatment of citrus pectin: this treatment lowers the molecular weight to between 5 and 10 kDa.

Chemical and enzymatic modification will reduce the molecular weight by preferentially cleaving the homogalacturonan. For GCS-100 alkali treatment of the pectin will cause β-elimination reactions resulting in depolymerisation of the homogalacturonan backbone and de-esterification of the pectin (Renard & Thibault, 1996). Acid treatment preferentially cleaves neutral sugars (Thibault, Renard, Axelos, Roger, & Crepeau, 1993) and such cleavage is considered to follow the order Ara > Gal > Rha. Both chemical and enzymatic treatment should lead to extracts containing lower molecular weight homogalacturonans and fragments enriched in rhamnogalacturonans.

Modification reduces the average molecular weight enhancing the solubility of the product. This treatment is also considered to enhance the accessibility and binding of MCP to Gal3. The early studies of Inohara and Raz (1994) showed that chemically modified citrus pectin (but not the original citrus pectin) bound Gal3, and the binding was inhibited by 50 mM lactose. Improved accessibility is supported by the observation that, whilst native citrus pectin will bind galacturonic acid-specific lectins (Benhamou, Kloepper, & Tuzun, 1998), heat treatment, alkali (and presumably enzymatic) treatment is needed to enable significant interaction with galactose-specific lectins (Koppitz, Woehlecke, & Ehwald, 1994; Luck, Ehwald, Ziska, & Koppitz, 1992). These studies suggest that the component most likely to bind to Gal3 is the enriched RGI or modified (arabinose-depleted) RGI. Recent biophysical studies (Gunning, Bongaerts, & Morris, 2009) showed that homogalacturonan (citrus) fragments did not bind specifically to Gal3 but that potato RGI and potato RGI, modified to remove arabinose, bound specifically to Gal3. RGI bound weakly and the binding was enhanced on removal of arabinose. The binding of the modified RGI to Gal3 was dose-dependent, inhibited by lactose, and force spectroscopy measurements of the detachment force suggested that binding occurred within the Gal3 carbohydrate recognition domain. Enzymatic studies (Obro, Harholt, Scheller, & Orfila, 2004) on the structure of potato RGI suggest that the RGI regions contain α(1 → 5)-linked arabinans and an abundance of β(1 → 4)-D-galactans, poorly substituted with arabinose. Thus potato RGI contains linear β(1 → 4) linked D-galactans similar to those present in citrus RGI, suggesting that the bioactivity of MCP that is attributed to inhibition of Gal3 arises from the galactan chains. The enhanced specific binding to Gal3 on removal of arabinose reinforces the idea that modification enhances the accessibility of the galactan chains to Gal3.

Binding of galactan chains to Gal3 will occur at the non-reducing end of the galactan chain and the entity binding within the CRD will be – ←1)-β-D-Gal (4 ←1)-β-D-Gal. Thus, in this study, we have investigated the binding of the disaccharide β-D-galactobiose to Gal3 using force spectroscopy. This technique allows interactions between individual molecules to be probed directly using relatively small amounts of materials and provides novel information on the nature and lifetime of the binding site. These studies have been used to demonstrate specific binding, and to characterise the nature of the binding to Gal3.

2. Materials and methods

Recombinant human Gal3 was purchased as a Gal3–lactose complex from Sigma Chemicals Ltd. (Lot # 087K1138, Poole, UK). Samples of β-galactobiose samples were obtained from Megazyme International Ireland Ltd. (Lot # 80501, Bray, Ireland). The remaining materials were purchased from Sigma Chemicals Ltd. (UK) unless otherwise stated.

2.1. Preparation of functionalised substrates

Silica beads and glass slides were used as substrates. The silica beads (mean diameter 6.8 μm) were purchased from Bangs Laboratories (Fishers, IN, USA). Beads were initially acid washed in hydrochloric acid (HCl)/methanol (MeOH) mixtures in order to regenerate surface hydroxyl groups (30 min in 1:1 HCl:MeOH), and cleaned prior to functionalisation by washing and then spinning down in a microcentrifuge through the following series: ultrapure water (3× 1 ml, 18.2 MΩ (Elga Ltd., Marlowe, UK), very low-residue ethanol (3× 1 ml (Fluka Chemicals, Poole, UK), and toluene (3× 1 ml, dried over molecular sieve 4 Å). Following each centrifugation cycle the supernatant was discarded. Functionalisation followed a protocol described by Bhatia et al. (1989). The silica beads were initially functionalised with a layer of 3-mercaptopropyltrimethoxy silane (MTS). For force spectroscopy studies the silanised beads were coated with 4-(4-N-maleimidophenyl) butyric acid hydrazide hydrochloride (MPBH, Pierce, Rockford, IL, USA): a carbohydrate coupling agent. The silanised beads were then glued onto the end of the AFM cantilevers (long thin NP; Veeco Inc., USA) using a 2-part epoxy resin (40 min cure time; Permatex Inc., USA). The tip was dipped into the liquid resin and then pressed down onto the bead. Once the epoxy resin had hardened the cantilever-bead assemblies were incubated with β-galactobiose solutions (2 mg ml^{-1}, 22 °C, in phosphate buffered saline (PBS), 1 h), rinsed in PBS and then incubated for 30 min in a 10 mg ml^{-1} glucose solution in PBS to cap any unreacted hydrazide sites on the bead, followed by rinsing in PBS. Finally the functionalised tips were inserted into the liquid cell of the AFM and maintained under a PBS solution.

MTS coated glass slides for force spectroscopy studies were functionalised with Gal3–lactose complexes attached via a heterobifunctional polyethylene glycol (PEG) spacer molecule (O-[N-(6-maleimidohexanoyl)aminoethyl]-O′-[3-(N-succinimidyloxy)-3-oxopropyl]polyethylene glycol 3000, Lot # 1292103, Sigma Chemicals, Poole, UK) to facilitate binding of the Gal3 to the small disaccharide molecules. One end of the PEG contains an n-hydroxy succinimide (NHS) ester which covalently binds primary amines at neutral pH, and the other end of the PEG contains a maleimido group which binds to the surface adsorbed thiol groups on the MTS coated glass slide. Selected regions of the functionalised slides were incubated with the Gal3–lactose complexes (0.1 mg ml^{-1} solutions of the lectin in PBS for 1 h at room temperature), washed in PBS, and incubated in a freshly prepared solution of 1 M hydroxylamine in PBS (titrated to pH 6.0 with NaOH) to cap any unreacted succinimide groups, rinsed in PBS and inserted into the AFM liquid cell. The multiple PBS washing steps will remove lactose from the Gal3 complexes and thus activate the Gal3 molecules.

2.2. Force spectroscopy

Force spectroscopy data was obtained using an MFP-3D AFM (Asylum Research, CA, USA). The carbohydrate-coated functionalised silica beads attached to the end of the AFM cantilevers were

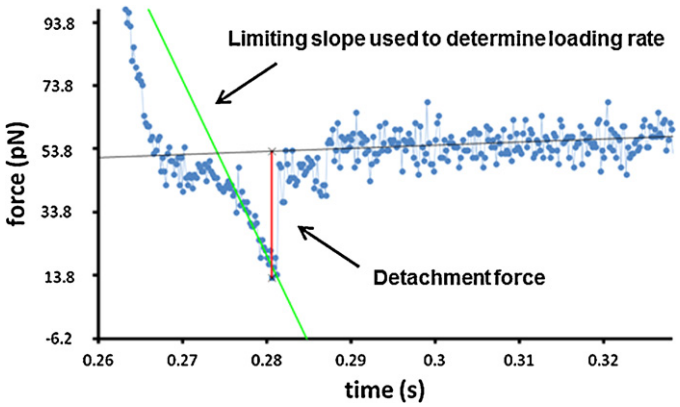

Fig. 1. Analysis of force versus time data for galactobiose–Gal3 rupture events.

pressed against Gal3-coated glass surfaces in order to probe β-galactobiose interactions. Measurements were made by ramping the AFM tip towards and then away from the sample surface under buffer solution (either pure PBS or a lactose solution in PBS) at a controlled speed (in the range 200–2000 nm s^{-1}). This process was repeated typically several hundred times for each tip-sample and solution combination at randomly selected points on the functionalised surface in order to generate statistics on the frequency and magnitude of adhesion. The measurement was further controlled by setting a maximum loading force of 300 pN in order to minimise damage to the functionalised bead at the end of the AFM cantilever, and a dwell period of 0.99 s was imposed on the tip-sample contact phase of the measurement in order to increase the chances of capturing binding events.

2.3. Analysis of force spectroscopy data

Tip-sample adhesion data were analysed by quantifying the magnitude of the negative adhesive peak following extension of the PEG spacer, seen upon retraction of the functionalised AFM tip from the functionalised sample surface.

Fig. 1 illustrates how the magnitude of the detachment force and the loading rate were determined from the retract portion of the force curves. The AFM used in this study allows the force data to be plotted directly against time. This provides much greater accuracy than the 'effective spring constant' method which multiplies the slope of force versus distance curve at the rupture point with the pulling speed set in the instrument software: this is an assumed speed which can be subject to error from several sources, such as non-linearity of the piezoelectric devices, creep and, most importantly at higher pulling speeds, hydrodynamic drag effects on the AFM cantilever (Webber et al., 2008). The loading rate at bond rupture was determined as the regression slope of those points following a linear pattern immediately before the rupture point. The magnitude of the rupture force was determined by quantifying the difference between force value at the rupture point and a linear fit extrapolated from the off region of the data. In order to eliminate ambiguous events, a limiting threshold for the magnitude of the rupture force was set at seven times the noise estimated as the root mean square error of the linear fit in the off region of the data. The resulting data was then assigned to bins in order to generate histograms depicting the distribution of values. Curve fitting was carried out with an in-house developed Excel add-in.

3. Results and discussion

The force spectroscopy studies were carried out in order to investigate potential specific binding of β-galactobiose to Gal3. Fig. 2a is a schematic diagram showing the attachment of the β-galactobiose-activated sphere to the tip-cantilever assembly and the attachment of Gal3 to the glass substrate via PEG spacer molecules. Fig. 2b shows an example of approach and retract curves, which reveal a specific interaction between β-galactobiose and Gal3: the curves show hysteresis between the advance and retract curves revealing evidence of a binding event on retraction. The retract curve in Fig. 2b shows a region corresponding to the extension of the flexible PEG spacer prior to the breakage of the β-galactobiose–Gal3 linkage. The presence of the PEG spacer facilitates binding of Gal3 to β-galactobiose by allowing the molecules geometrical freedom, and its defined molecular weight helps to distinguish between specific and non-specific binding events.

On approach the cantilever deflection remains constant until the sphere and substrate come into contact. On retraction non-specific interactions will show up at this point of contact if the derivatised AFM tip adheres to the substrate surface. Specific binding events between the carbohydrate and protein are by contrast, shifted along the horizontal axis, by a distance that depends on the contour length of the PEG spacer, and these events will be preceded by a characteristic non-linear peak due to stretching of the PEG. The example curve shown in Fig. 2b shows both hallmarks of specific binding, suggesting it represents interaction of β-galactobiose with Gal3.

In the present study a series of force versus distance curves were recorded and exhibited an adhesive event rate of some 10%, which according to previous studies is optimal for capturing single-molecule unbinding spectra (Hinterdorfer and Dufrêne, 2006). Ligand–receptor binding is an equilibrium process and thus controlled addition of the inhibitor lactose can be used to inactivate a high proportion of the immobilised Gal3 molecules. When done for the present system the percentage of adhesive events obtained fell to 0.5%. The original distribution of adhesion events was recovered upon rinsing with PBS in order to remove lactose. The effect of addition of lactose in inhibiting the binding of β-galactobiose to Gal3 confirms that the binding occurs within the carbohydrate recognition domain.

Force spectroscopy studies yielded a range of detachment forces (Fig. 3). The modal value of the measured detachment force (35 pN) is typical of that observed for other carbohydrate–lectin interactions (Dettmann et al., 2000; Gunning et al., 2009; Touhami, Hoffmann, Vasella, Denis, & Dufrene, 2003a,b), suggesting again that there is a specific interaction between β-galactobiose and Gal3 which involves binding into the carbohydrate recognition domain.

Touhami et al. (2003a,b) reported a value of 96 pN for single carbohydrate interactions between glucose and Concanavalin A and a similar value (121 pN) for single interactions between glucose and individual glucose-binding lectins expressed on the surface of live yeast cells. Previous force spectroscopy studies (Gunning et al., 2009) on the interaction of arabinose-depleted pectin-derived RGI and Gal3 reported a modal detachment force for single intermolecular interactions of 79 pN. Studies on lactose–galectin 1 interactions (Dettmann et al., 2000) reported that the detachment force varied with loading rate, and a measured detachment force of 34 pN was reported at a loading rate of 3 nN s^{-1}. Although it is tempting to conclude that the higher detachment force for the modified RGI indicates stronger binding for the galactan chains than for β-galactobiose, the variation of the detachment force with loading rate means that it is not possible to easily use the relative values of the measured detachment forces to gauge the relative inhibitory effects of different oligosaccharides.

The dependence of the detachment force on loading rate arises because of the kinetic nature of the binding between carbohydrates and lectins (Lee, Wang, Huang, & Lin, 2007). At very slow loading rates the interaction between the lectin and the carbohydrate ligand will have sufficient time to dissociate, and the measured

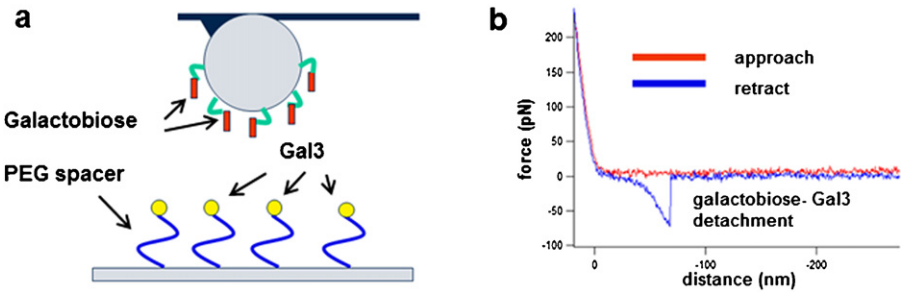

Fig. 2. Force spectroscopy studies of Gal3 and β-galactobiose interactions. (a) Schematic diagram showing the activated substrate and activated spheres attached to the AFM cantilever. (b) Approach and retract curves showing the detachment of the β-galactobiose from Gal3.

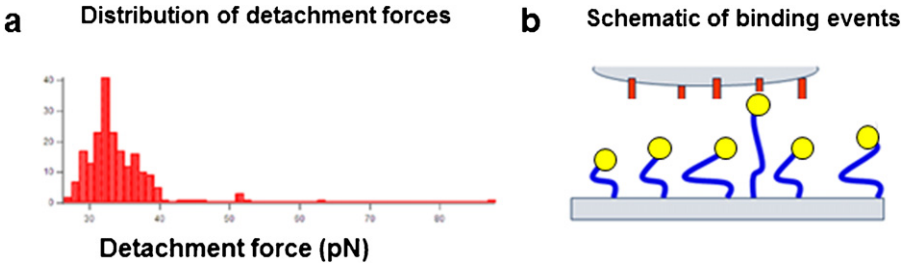

Fig. 3. Gal3–β-galactobiose binding. (a) Distribution of measured detachment values corresponding to single molecule events. (b) Schematic of the binding events.

detachment force will be zero. Thus, by extrapolating the measured detachment forces to slower loading rate it is possible to analyse the data to determine a lifetime for the carbohydrate–lectin interaction.

Fig. 4 shows a comparison of two individual force–time curves obtained from the present study. From the measured asymptotic slope (df/dt) of the force–time retract curve as it reaches the point of detachment, it is possible to measure the loading rate on detachment. For the two curves shown it is clear that the measured detachment force decreased with decreased loading rate on detachment.

Such variation demonstrates why quoting single values for detachment force in ligand–receptor systems is of limited utility if it is not accompanied by information on the actual loading rate at bond rupture, and that a better approach is to model the interaction between the component parts in order to compare data for different ligands. The relationship between loading rate and bond rupture force has been studied in detail by Evans and Richie (1997, 1999). Fig. 5 shows a plot of the measured detachment force (f) as a function of the logarithm of the loading rate, $ln\{r\}$. Over the range of detachment forces measured in the present study the plot of f versus $ln\{r\}$ was linear. The fitted line is a least squares fit to the data shown in the histogram (Fig. 3a), which includes all measured detachment forces for which the measured force was at least seven times greater than the noise level on the retract curve. Strunz, Oroszlan, Schumakovitch, Güntherodt, and Hegner (2000) have derived an expression for the dependence of the most probable binding force, the modal value f^*, on loading rate (r) of the form:

$$f^* = \frac{k_B T}{x} \, ln \, \frac{rx}{k_B T k_{off}}$$

where k_B is the Boltzmann constant and k_{off} is the dissociation rate at zero applied force. x is parameter introduced by Bell (1978) which characterises the energy landscape: x is effectively the distance the bond has to be stretched along a reaction coordinate in order to dissociate the molecules.

The measured detachment forces span f^* and define the slope $df/d(ln(r)) = k_B T/x$ at $f = f^*$ yielding $x = 0.2$ nm. The parameter k_{off} can then be determined from known values of f^* and the loading rate (r^*) at $f = f^*$, or from the intercept on the $ln\{r\}$ axis at $f = 0$. This yields a value for $k_{off} = 0.33\ s^{-1}$ and a lifetime for the interaction of 3.0 s.

These studies confirm that the terminal disaccharide (β-galactobiose) at the non-reducing end of β(1 → 4)-D-galactan

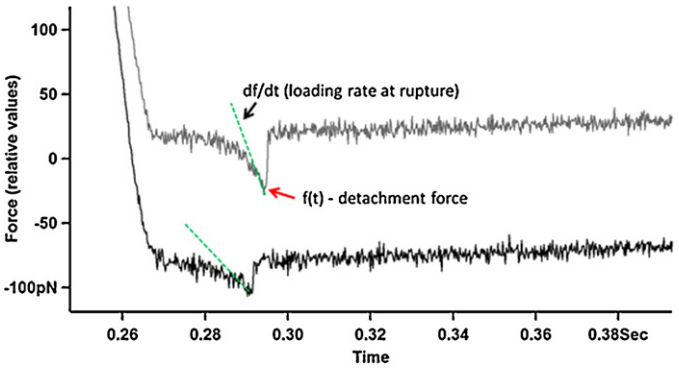

Fig. 4. Comparison of isolated force-distance curves for β-galactobiose–Gal3 interactions. These two curves illustrate a decreased detachment force for a decreased loading rate.

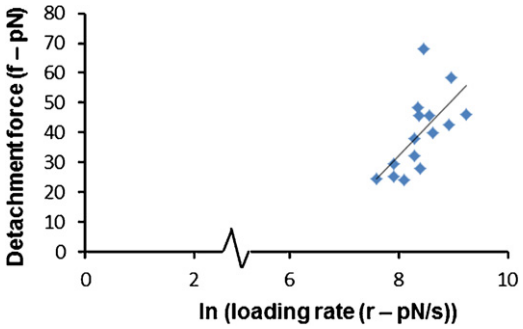

Fig. 5. Plot of detachment force (f) versus the logarithm of the loading rate $ln\{r\}$ for the Gal3–β-galactobiose interactions.

sidechains will bind specifically to Gal3 and suggest a lifetime for the interaction of 3.0 s.

4. Conclusions

Force spectroscopy studies have revealed a specific interaction between β-galactobiose and Gal3. β-Galactobiose is the terminal disaccharide of the β(1 → 4)-D-galactan sidechains within the RGI regions of citrus pectin. The binding is inhibited by lactose, suggesting binding within the carbohydrate recognition domain of Gal3. The measured detachment force is characteristic of the values observed for carbohydrate–lectin interactions. Analysis of the dependence of the detachment force on the measured loading rate at detachment suggest a dissociation rate for the interaction at zero force of $k_{off} = 0.33\ s^{-1}$ and a lifetime for the interaction of 3.0 s. The data is consistent with the hypothesis that oral consumption of MCP controls cancer metastasis by inhibiting the role of the pro-metastatic regulatory protein Gal3. The modification is considered to promote uptake and enhance accessibility of these sidechains for binding to Gal3.

Acknowledgement

The research described in this article was funded by the Biotechnology and Biological Science Research Council (BBSRC) through the core grant to IFR.

References

Barondes, S. H., Castronovo, V., Cooper, D. N. W., Cummings, R. D., Drickmer, K., Feizi, T., et al. (1994). Galectins – A family of animal β-galactoside-binding lectins. *Cell*, *76*, 597–598.

Barondes, S. H., Cooper, D. N. W., Gitt, M. A., & Leffler, H. (1994). Galectins-structure and function of a large family of animal lectins. *Journal of Biological Chemistry*, *269*, 20807–20810.

Bell, G. I. (1978). Models for the specific adhesion of cells to cells. *Science*, *200*, 618–627.

Benhamou, N., Kloepper, J. W., & Tuzun, S. (1998). Induction of resistance against *Fusarium* wilt of tomato by combination of chitosan with an endophytic bacterial strain: Ultrastructure and cytochemistry of the host response. *Planta*, *204*, 153–168.

Bhatia, S. K., Shriverlake, L. C., Prior, K. J., George, J. H., Calvert, J. M., Bredhorst, R., et al. (1989). Use of thiol-terminal silanes and heterobifunctional crosslinkers for immobilization of antibodies on silica surfaces. *Analytical Biochemistry*, *178*, 408–413.

Birdsall, B., Feeney, J., Burdett, I. D. J., Bawumia, S., Barboni, E. A. M., & Hughes, R. C. (2001). NMR solution studies of hamster galectin-3 and electron microscopic visualisation of surface-adsorbed complexes: Evidence for interactions between the N- and C-terminal domains. *Biochemistry*, *40*, 4859–4866.

Collins, P., Hidari, K. I. P. J., & Blanchard, H. (2007). Slow diffusion of lactose out of galectin-3 crystals monitored by X-ray crystallography: Possible implications for ligand-exchange protocols. *Acta Crystallography*, *D63*, 415–419.

Dettmann, W., Grandbois, M., André, S., Benoit, M., Angelika, K., Wehle, A. K., et al. (2000). Differences in zero-force and force-driven kinetics of ligand dissociation from beta-galactoside-specific proteins (plant and animal lectins, immunoglobulin G) monitored by plasmon resonance and dynamic single molecule force microscopy. *Archives of Biochemistry and Biophysics*, *383*, 157–170.

Evans, E., & Richie, K. (1997). Dynamic strength of molecular adhesion bonds. *Biophysical Journal*, *72*, 1541–1555.

Evans, E., & Richie, K. (1999). Strength of a weak bond connecting flexible polymer chains. *Biophysical Journal*, *76*, 2439–2447.

Glinsky, V. V., & Raz, A. (2009). Modified pectin anti-metastatic properties: One bullet, multiple targets. *Carbohydrate Research*, *344*, 1788–1791.

Gunning, A. P., Bongaerts, R. J. M., & Morris, V. J. (2009). Recognition of galactan components of pectin by galectin-3. *The FASEB Journal*, *23*(2), 415–424.

Hinterdorfer, P., & Dufrêne, Y. F. (2006). Detection and localization of single molecular recognition events using atomic force microscopy. *Nature Methods*, *3*, 347–355.

Inohara, H., & Raz, A. (1994). Effects of natural complex carbohydrate (citrus pectin) on murine melanoma cell properties related to galectin-3 functions. *Glycoconjugate Journal*, *11*(6), 527–532.

Koppitz, H., Woehlecke, H., & Ehwald, R. (1994). Crosslinking treatment for increasing lectin binding capacity of a vesicular affinity sorbent consisting of higher plant cell walls. *Phytochemistry*, *35*, 1205–1213.

Lee, C.-H., Wang, Y.-M., Huang, L. S., & Lin, S. (2007). Atomic force microscopy: Determination of unbinding force, off rate and energy barrier for protein–ligand interaction. *Micron*, *38*, 446–461.

Luck, K., Ehwald, R., Ziska, P., & Koppitz, H. (1992). Affinity sorbent for galactose specific lectins consisting of deproteinized plant cell wall ghosts. *Plant Science*, *82*, 29–35.

Nesmelova, I. V., Dings, R. P. M., & Mayo, K. H. (2008). Understanding galectin structure–function relationships to design effective antagonists. In A. A. Klyosov, Z. J. Witczak, & D. Platt (Eds.), *Galectins* (pp. 33–69). NJ, USA: J. Wiley & Sons.

Obro, J., Harholt, J., Scheller, H. V., & Orfila, C. (2004). Rhamnogalacturonan I in *Solanum tuberosum* tubers contains complex arabinogalactan structures. *Phytochemistry*, *65*, 1429–1438.

Raz, A., & Pienta, K. J. (1998). *Method for inhibiting cancer metastasis by oral administration of soluble modified citrus pectin*. US patent number 5,834,442.

Renard, C. M. G. C., & Thibault, J.-F. (1996). Degradation of pectins in alkaline conditions: Kinetics of demethylation. *Carbohydrate Research*, *286*, 139–150.

Ridley, B. L., O'Neill, M. A., & Mohnen, D. (2001). Pectins: Structure, biosynthesis, and oligogalacturonide-related signaling. *Phytochemistry*, *57*(6), 929–967.

Seetharaman, J., Kanigsberg, A., Slaaby, R., Leffler, H., Barondes, S. H., & Rini, J. M. (1998). X-ray crystal structure of the human galectin-3 carbohydrate recognition domain at 2.1-angstrom resolution. *Journal of Biological Chemistry*, *273*, 13047–13052.

Sörme, P., Arnoux, P., Kahl-Knutsson, B., Leffler, H., Rini, J. M., & Nilsson, L. J. (2005). Structural and thermodynamic studies on cation-II interactions in lectin–ligand complexes: High-affinity galectin-3 inhibitors through fine-tuning of an arginine-arene interaction. *Journal of the American Chemical Society*, *127*, 1737–1743.

Strunz, T., Oroszlan, K., Schumakovitch, I., Güntherodt, H.-J., & Hegner, M. (2000). Model energy landscapes and the force-induced dissociation of ligand–receptor bonds. *Biophysical Journal*, *79*, 1206–1212.

Thibault, J.-F., Renard, C. M. G. C., Axelos, M., Roger, P., & Crepeau, M. J. (1993). Studies of the length of homogalacturonic regions in pectins by acid-hydrolysis. *Carbohydrate Research*, *238*, 271–286.

Touhami, A., Hoffmann, B., Vasella, A., Denis, F., & Dufrene, Y. F. (2003a). Probing specific lectin–carbohydrate interactions using atomic force microscopy imaging and force measurements. *Langmuir*, *19*, 1745–1751.

Touhami, A., Hoffmann, B., Vasella, A., Denis, F., & Dufrene, Y. F. (2003b). Aggregation of yeast cells: Direct measurement of discrete lectin–carbohydrate interactions. *Microbiology*, *149*, 2873–2878.

Wang, Y., Nangia-Makker, P., Balan, V., & Raz, A. (2010). Calpain activation through galectin-3 inhibition sensitizes prostate cancer cells to cisplatin treatment. *Cell Death and Disease*, *1* http://dx.doi.org/10.1038/cddis.2010.79, article number e101

Webber, G. B., Edwards, S. A., Stevens, G. W., Grieser, F., Dagastine, R. R., & Chan, D. Y. C. (2008). Measurements of dynamic forces between drops with the AFM: Novel considerations in comparisons between experiment and theory. *Soft Matter*, *4*, 1270–1278.

Yapo, B. M., Lerouge, P., Thibault, J.-F., & Ralet, M. C. (2007). Pectins from citrus peel cell walls contain homogalacturonans homogeneous with respect to molar mass, rhamnogalacturan I and rhamnogalacturonan II. *Carbohydrate Polymers*, *69*, 426–435.